Contribution from the Department of Chemistry and Biochemistry, University of Colorado, Boulder, Colorado 80309

Charge Distribution in the Quinone Complexes of Osmium: Synthesis and Characterization of the $Os(PPh_3)_2(Q)Cl_2$ and $Os(PPh_3)_2(Q)_2$ (Q = 3,5-Di-*tert*-butyl-1,2-quinone, Tetrachloro-1,2-quinone) Series

Samaresh Bhattacharya and Cortlandt G. Pierpont*

Received January 3, 1991

Members of the $Os(PPh_3)_2(Q)Cl_2$ and $Os(PPh_3)_2(Q)_2$ (Q = DBQ, Cl_4Q) families have been studied in order to understand the charge distribution in the neutral quinone complexes of osmium. The $Os(PPh_3)_2(Q)Cl_2$ complexes have been synthesized by the reaction of $Os(PPh_3)_3Cl_2$ with BQ (BQ = DBBQ, Cl_4BQ). $Os(PPh_3)_2(DBQ)Cl_2$ has been characterized structurally. Crystals of $Os(PPh_3)_2(DBQ)Cl_2$ form in the monoclinic space group $P2_1/c$ with $Z = 4$ in a unit cell of dimensions, $a = 16.504$ (3) Å, $b = 12.206$ (3) Å, $c = 22.563$ (3) Å, and $\beta = 100.63$ (10)°. Structural features of the quinone ligand indicate that in the solid state it is intermediate between semiquinone and catechol. Treatment of $Os(PPh_3)_2(Q)Cl_2$ with a second catecholate ligand leads to displacement of the chloro ligands with formation of the bis(quinone) product. The $Os(PPh_3)_2(Q)_2$ complexes have also been synthesized by the reaction of $Os(PPh_3)_3Cl_2$ with H_2Cat ($H_2Cat = H_2DBCat$, H_2Cl_4Cat). $Os(PPh_3)_2(DBQ)_2$ has been characterized crystallographically. Crystals of this compound form in the monoclinic space group $P2_1/n$ with $Z = 4$ in a unit cell of dimensions $a = 13.539$ (2) Å, $b = 15.629$ (4) Å, $c = 27.105$ (7) Å, and $\beta = 100.21$ (2)°. Structural features of the quinone ligands are both typically catecholate. Electrochemical characterization has shown that each of the two $Os(PPh_3)_2(Q)Cl_2$ complexes undergoes one oxidation and one reduction at potentials similar to those observed for the $Ru(PPh_3)_2(SQ)Cl_2$ complex. The bis(quinone)osmium complexes show redox behavior similar to that of the $Ru(PPh_3)_2(SQ)_2$ complexes. This similarity indicates that in solution the $Os(PPh_3)_2(Q)Cl_2$ and $Os(PPh_3)_2(Q)_2$ complexes have electronic structures similar to those of members of the $Ru(PPh_3)_2(SQ)Cl_2$ and $Ru(PPh_3)_2(SQ)_2$ series, respectively.

Introduction

There has been significant current interest in the chemistry of transition-metal complexes of orthoquinone ligands. These ligands can bind metal atoms in three different electronic forms, viz. benzoquinone, semiquinonate, and catecholate.[1] Electron distribution in complexes containing quinone ligands is sensitive to the orbital energy of metal valence electronic levels. Distinct variations in charge distribution have been noted for first-row metals relative to complexes containing larger members of a group.[2] Among the tris(quinone) complexes of the Cr, Mo, W triad, chromium complexes are of the form $Cr^{III}(SQ)_3$,[3] while related complexes of the larger metals are of the form $M^{VI}(Cat)_3$ (M = Mo, W).[4] The iron triad has been of particular interest because the metals of this group, particularly Ru and Os, have valence levels that are close in energy to the quinone π-level.[2,5] This results in apparent delocalization within the Ru–quinone and Os–quinone chelate rings and ambiguity in charge distribution.[6] Although the coordination chemistry of congeneric metals of the second- and third-transition series is generally regarded to be quite similar, charge distributions in the complexes $Ru(DBQ)_3$ and $Os(DBQ)_3$ are different.[2] In the Os complex the metal is more oxidized and the ligands are more catechol-like relative to the Ru complex. The same trend has been observed for the $[M(bpy)_2(DBQ)]^+$ (M = Ru, Os) complexes.[6,7] The average C–O bond length (1.308 Å) is more semiquinone-like for $Ru(bpy)_2(DBSQ)^+$; however, for $Os(bpy)_2(DBCat)^+$, the average C–O bond length (1.346 Å) is typical of a catecholate ligand. Spectral and electrochemical properties of members of the $M(bpy)_2Q^n$ series (M = Ru, Os; $n = +1, 0, -1$) show evidence of M–Q delocalization, complicating assignment of formal charges. Recently, we reported a series of mixed-ligand Ru–quinone complexes of general form $Ru(PPh_3)_2(Q)Cl_2$ and $Ru(PPh_3)_2(Q)_2$.[8] Structural features of $Ru(PPh_3)_2(DBSQ)Cl_2$ revealed that the quinone ligand is in the semiquinonate form and the metal is trivalent. Structural features of $Ru(PPh_3)_2(ClSQ)_2$ indicated that, in the bis(quinone) Ru complexes, the metal is bivalent and the ligands are in the semiquinonate form in the solid. Marked similarities in solution electronic spectra and electrochemical properties of corresponding members of the $Ru(bpy)Q_2$ and $Ru(PPh_3)_2Q_2$ series showed that the valence electronic levels of these complexes were insensitive to differences in counterligand bonding effects. These observations were interpreted to indicate that the electronic levels associated with these properties, the frontier orbitals of the complex, are predominantly quinone ligand in character. In the present paper, we will describe the synthesis, characterization, and electronic description of the members of the $Os(PPh_3)_2(Q)Cl_2$ and the $Os(PPh_3)_2(Q)_2$ (Q = Cl_4Q, DBQ) families.

Experimental Section

Materials. Osmium(III) chloride hydrate ($OsCl_3 \cdot nH_2O$), triethylamine (NEt_3), triphenylphosphine (PPh_3), 3,5-di-*tert*-butylcatechol (H_2DBCat), 3,5-di-*tert*-butyl-1,2-benzoquinone (DBBQ), and 3,4,5,6-tetrachloro-1,2-benzoquinone (Cl_4BQ) were purchased from Aldrich. Tetrachlorocatechol (H_2Cl_4Cat) was prepared by a published procedure and sublimed before use.[9]

Preparation of Complexes. $Os(PPh_3)_3Cl_2$. $OsCl_3 \cdot nH_2O$ (0.5 g, 1.69 mmol) and PPh_3 (2.5 g, 9.54 mmol) were refluxed in 50 mL of a 4:1 *tert*-butyl alcohol–water solvent mixture for 24 h under nitrogen. The mixture was allowed to cool to room temperature. The pale green solid was collected by filtration, washed thoroughly with ethanol, and dried in air. The yield was 1.4 g, 79%.

$Os(PPh_3)_2(DBQ)Cl_2$. Degassed dichloromethane (50 mL) was added to a mixture of $Os(PPh_3)_3Cl_2$ (500 mg, 0.48 mmol) and DBBQ (120 mg, 0.55 mmol) under N_2. The resulting solution became green almost immediately. The mixture was stirred for 4 h at room temperature, solvent was then evaporated under nitrogen, and the solid residue was washed thoroughly with hexane. Recrystallization from dichloromethane–hexane solution afforded dark green crystals of $Os(PPh_3)_2(DBQ)Cl_2$ (370 mg) in 77% yield.

$Os(PPh_3)_2(Cl_4Q)Cl_2$. This compound was synthesized in 75% yield by following the procedure described above using Cl_4BQ instead of DBBQ.

$Os(PPh_3)_2(DBQ)_2$: Procedure 1. H_2DBCat (50 mg, 0.23 mmol) was added to a suspension of $Os(PPh_3)_3Cl_2$ (100 mg, 0.10 mmol) in warm EtOH (50 mL). It was gently refluxed for 4 h with constant stirring. Within 30 min, the color of the solution became purple. Solvent was then

(1) Pierpont, C. G.; Buchanan, R. M. *Coord. Chem. Rev.* **1981**, *38*, 44.
(2) Bhattacharya, S.; Boone, S. R.; Fox, G. A.; Pierpont, C. G. *J. Am. Chem. Soc.* **1990**, *112*, 1088.
(3) Buchanan, R. M.; Kessel, S. L.; Downs, H. H.; Pierpont, C. G.; Hendrickson, D. N. *J. Am. Chem. Soc.* **1978**, *100*, 7894.
(4) (a) Cass, M. E.; Pierpont, C. G. *Inorg. Chem.* **1986**, *25*, 122. (b) deLearie, L. A.; Pierpont, C. G. *Inorg. Chem.* **1988**, *27*, 3842.
(5) Lever, A. B. P.; Auburn, P. R.; Dodsworth, E. S.; Haga, M.; Liu, W.; Melnik, M.; Nevin, W. A. *J. Am. Chem. Soc.* **1988**, *110*, 8076.
(6) (a) Haga, M.; Dodsworth, E. S.; Lever, A. B. P. *Inorg. Chem.* **1986**, *25*, 447. (b) Boone, S. R.; Pierpont, C. G. *Inorg. Chem.* **1987**, *26*, 1769.
(7) Haga, M.; Isobe, K.; Boone, S. R.; Pierpont, C. G. *Inorg. Chem.* **1990**, *29*, 3975.
(8) Bhattacharya, S.; Pierpont, C. G. *Inorg. Chem.* **1991**, *30*, 1511.
(9) Jackson, L. C.; MacLaurin, R. D. *J. Am. Chem. Soc.* **1988**, *110*, 8076.

0020-1669/91/1330-2906$02.50/0

Table I. Crystallographic Data for $Os(PPh_3)_2(DBQ)Cl_2$ and $Os(PPh_3)_2(DBQ)_2$

	$Os(PPh_3)_2(DBQ)Cl_2$	$Os(PPh_3)_2(DBQ)_2$
mol wt	1005.9	1155.3
color	green	purple
space group	$P2_1/c$	$P2_1/n$
a, Å	16.504 (3)	13.539 (2)
b, Å	12.206 (3)	15.629 (4)
c, Å	22.563 (3)	27.105 (7)
β, deg	100.63 (10)	100.21 (2)
vol, Å^3	4467.3 (14)	5645.0 (2)
Z	4	4
D_{calcd}, g cm^{-3}	1.496	1.359
D_{expt}, g cm^{-3}	1.493	1.358
μ, mm^{-1}	3.086	2.361
λ, Å	0.71073 (Mo Kα)	
T, °K	295–297	
R, %; R_w(obsd data), %	2.53; 3.57	2.91; 3.60
GOF	0.95	0.86

Table II. Selected Atomic Coordinates for $Os(PPh_3)_2(DBQ)Cl_2$

	x/a	y/b	z/c
Os	2834 (1)	1373 (1)	1466 (1)
Cl1	4230 (1)	1349 (1)	1387 (1)
Cl2	2302 (1)	1803 (1)	454 (1)
P1	2763 (1)	−542 (1)	1179 (1)
P2	2895 (1)	3304 (1)	1709 (1)
O1	3169 (2)	914 (3)	2317 (1)
O2	1724 (2)	1377 (2)	1747 (1)
C1	2569 (3)	764 (4)	2619 (2)
C2	1763 (3)	1055 (4)	2316 (2)
C3	1092 (3)	999 (4)	2627 (2)
C4	1280 (3)	607 (4)	3211 (2)
C5	2073 (3)	287 (5)	3512 (2)
C6	2716 (3)	368 (4)	3206 (2)
C7	219 (3)	1410 (5)	2371 (3)
C11	2195 (3)	−130 (6)	4164 (3)

allowed to evaporate in air. The solid residue was dissolved in a small volume of benzene and filtered to remove any insoluble material. This filtrate was chromatographed on an alumina column using benzene as eluant. The major purple band, which came out first, was collected and evaporated to give dark purple crystals of $Os(PPh_3)_2(DBQ)_2$ (80 mg) in 73% yield.

$Os(PPh_3)_2(DBQ)_2$: Procedure 2. A solution of H_2DBCat (24 mg, 0.11 mmol) in EtOH (40 mL) was added to a warm solution of $Os(PPh_3)_2(DBQ)Cl_2$ (80 mg, 0.08 mmol) in CH_2Cl_2 (15 mL). The mixture was stirred for 15 min, NEt_3 (0.5 mL) was added, and the mixture was gently refluxed for 5 h with constant stirring. Within 30 min, the color of the solution turned purple. It was then cooled to room temperature and filtered. The filtrate was evaporated in air and the solid residue was washed with hexane, dissolved in benzene, filtered, and chromatographed as above. $Os(PPh_3)_2(DBQ)_2$ (64 mg) was obtained as a dark purple solid in 70% yield.

$Os(PPh_3)_2(Cl_4Q)_2$. This compound was prepared in 70% yield by following procedure 1 above using H_2Cl_4Cat instead of H_2DBCat.

$Os(PPh_3)_2(DBQ)(Cl_4Q)$. This complex was synthesized in 65% yield by following procedure 2 above using H_2Cl_4Cat instead of H_2DBCat.

Physical Measurements. Electronic spectra were recorded on a Perkin-Elmer Lambda 9 spectrophotometer. Infrared spectra were obtained on an IBM IR/30 FTIR spectrometer with samples prepared as KBr pellets. ^1H NMR spectra were recorded on a Varian VXR 300S spectrometer. Cyclic voltammograms were obtained with a Cypress CYSY-1 computer-controlled electroanalytical system. A platinum-disk working electrode and a platinum-wire counter electrode were used. A Ag/Ag^+ reference electrode was used that consisted of a CH_3CN solution of $AgPF_6$ in contact with a silver wire placed in glass tubing with a Vycor frit at one end to allow ion transport. Tetrabutylammonium perchlorate (TBAP) was used as the supporting electrolyte, and the ferrocene/ferrocenium couple was used as the internal standard.[10]

(10) The electrochemical properties of the $Ru(PPh_3)_2(Q)_2$ (Q = DBQ, Cl_4Q) series were reported previously. These experiments were carried out in CH_3CN solution. The limited solubility of members of the $Os(PPh_3)_2(Q)_2$ series in CH_3CN has required that experiments be carried out in CH_2Cl_2. For purposes of comparison, cyclic voltammograms on members of the $Ru(PPh_3)_2(Q)_2$ series have been reinvestigated in CH_2Cl_2, giving the potentials listed in Table VI.

Table III. Selected Atomic Coordinates for $Os(PPh_3)_2(DBQ)_2$

	x/a	y/b	z/c
Os	2334 (1)	1812 (1)	1018 (1)
P1	2668 (1)	406 (1)	1317 (1)
P2	943 (1)	2109 (1)	1399 (1)
O1	1351 (3)	1664 (3)	379 (2)
O2	3290 (3)	1658 (3)	518 (2)
O3	3453 (3)	2155 (3)	1556 (2)
O4	2436 (3)	3077 (3)	846 (2)
C1	1774 (4)	1901 (4)	−5 (2)
C2	2828 (4)	1879 (4)	65 (2)
C3	3331 (5)	2032 (4)	−346 (3)
C4	2731 (5)	2250 (4)	−787 (3)
C5	1677 (5)	2319 (4)	−871 (3)
C6	1213 (5)	2135 (4)	−471 (3)
C7	4474 (5)	1965 (5)	−289 (3)
C11	1112 (6)	2574 (5)	−1385 (3)
C15	3941 (5)	2819 (4)	1397 (3)
C16	3370 (5)	3338 (4)	1020 (2)
C17	3783 (5)	4112 (4)	877 (3)
C18	4786 (5)	4259 (4)	1084 (3)
C19	5369 (5)	3726 (5)	1429 (3)
C20	4936 (5)	3011 (4)	1602 (2)
C21	3165 (5)	4741 (4)	515 (3)
C25	6483 (6)	3945 (5)	1601 (3)

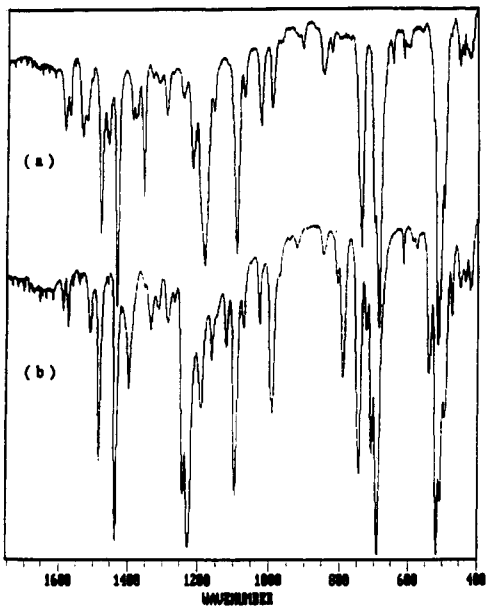

Figure 1. Infrared spectra of (a) $Os(PPh_3)_2(DBQ)Cl_2$ and (b) $Os(PPh_3)_2(Cl_4Q)Cl_2$.

Crystallographic Structure Determinations. $Os(PPh_3)_2(DBQ)Cl_2$. Dark green crystals of $Os(PPh_3)_2(DBQ)Cl_2$ were obtained by slow evaporation of a CH_2Cl_2–hexane solution of the complex. Axial photographs indicated monoclinic symmetry, and the centered settings of 25 reflections in the 2θ range between 20.6 and 33.2° gave the unit cell dimensions listed in Table I. Data were collected by θ–2θ scans within the angular range 3.0–45.0°. The location of Os was determined from a Patterson map and the positions of other atoms of the structure was determined from the phases generated by the heavy atoms. Final cycles of least-squares refinement converged with discrepancy indices of R = 0.025 and R_w = 0.036. Final positional parameters for selected atoms of the structure are contained in Table II. Tables containing full listings of atom positions, anisotropic thermal parameters, and hydrogen atom locations are available as supplementary material.

$Os(PPh_3)_2(DBQ)_2$. Purple crystals of $Os(PPh_3)_2(DBQ)_2$ were grown by slow evaporation of an ethanol–acetone solution of the compound. Monoclinic symmetry was indicated by axial photographs. The centered settings of 25 reflections in the 2θ range 19.4–30.4° afforded the unit cell dimensions given in Table I. Data collection, structure solution, and refinement were carried out as described above. Final cycles of refinement converged with discrepancy indices of R = 0.029 and R_w = 0.036. Final positional parameters for selected atoms of the structure are contained in Table III. Tables containing full listings of atom positions, anisotropic thermal parameters and hydrogen atom locations are available as supplementary material.

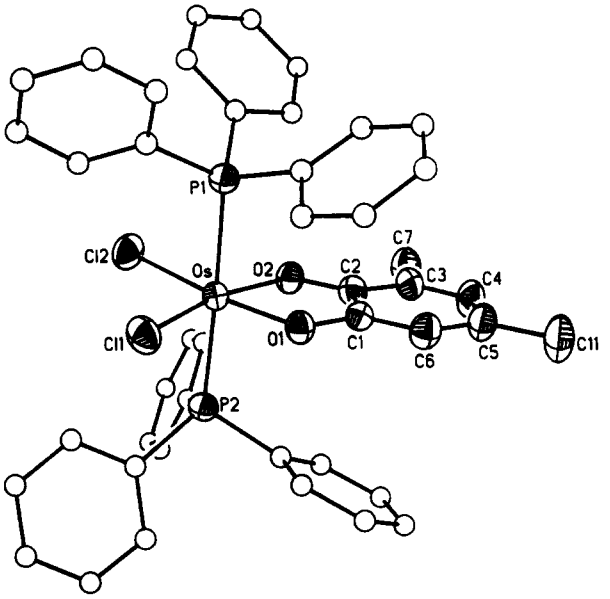

Figure 2. View of the $Os(PPh_3)_2(DBQ)Cl_2$ complex molecule.

Table IV. Selected Bond Distances and Angles for $Os(PPh_3)_2(DBQ)Cl_2$

	Distances (Å)		
Os–O1	1.980 (3)	C2–O2	1.333 (6)
Os–O2	2.047 (3)	C1–C2	1.425 (6)
Os–P1	2.422 (1)	C2–C3	1.418 (7)
Os–P2	2.418 (1)	C3–C4	1.381 (7)
Os–Cl1	2.344 (1)	C4–C5	1.414 (7)
Os–Cl2	2.348 (1)	C5–C6	1.372 (7)
C1–O1	1.312 (6)	C6–C1	1.389 (7)
	Angles (deg)		
Cl1–Os–Cl2	97.2 (1)	Cl1–Os–P1	88.1 (1)
Cl2–Os–P1	88.0 (1)	Cl1–Os–P2	91.7 (1)
Cl2–Os–P2	89.7 (1)	P1–Os–P2	177.7 (1)
Cl1–Os–O1	88.2 (1)	Cl2–Os–O1	173.6 (1)
P1–Os–O1	88.7 (1)	P2–Os–O1	93.6 (1)
Cl1–Os–O2	166.5 (1)	Cl2–Os–O2	96.1 (1)
P1–Os–O2	94.8 (1)	P2–Os–O2	85.9 (1)
O1–Os–O2	78.7 (1)		

Experimental Results

$Os(PPh_3)_2(DBQ)Cl_2$. $Os(PPh_3)_3Cl_2$ reacts smoothly with DBBQ in dichloromethane to afford $Os(PPh_3)_2(DBQ)Cl_2$ with the displacement of one triphenylphosphine ligand. The complex is diamagnetic and displays sharp *tert*-butyl resonances for the quinone ligand. Three intense resonances at 0.595, 1.036, and 2.253 ppm, of approximate intensity ratio 2:1:1, indicating superposition of two resonances at 0.595 ppm, are observed, corresponding to two isomers of the complex. Three localized charge distributions are possible for this complex, viz. Os^{II}–BQ, Os^{III}–SQ, Os^{IV}–Cat. The IR spectrum of the complex (Figure 1) does not show the high-energy C=O vibrations, which are typical of the unreduced DBBQ ligand eliminating the Os^{II}–BQ charge distribution. The analogous ruthenium complex $Ru(PPh_3)_2(DBSQ)Cl_2$ is also diamagnetic and has been structurally characterized.[8] Ligand C–O lengths were found to be consistent with a Ru^{III}–SQ charge distribution. $Os(PPh_3)_2(DBQ)Cl_2$ has also been characterized by X-ray crystallography. A view of the $Os(PPh_3)_2(DBQ)Cl_2$ molecule is shown in Figure 2 and selected bond distances and angles are given in Table IV. The two PPh_3 ligands are trans to one another in the complex molecule. Features of the quinone ligand do not point to a definite charge distribution. The average C–O bond length in this complex is 1.323 (11) Å, which is slightly longer than the average C–O bond length of 1.302 (4) Å in the analogous Ru complex, yet shorter than the typical C–O length of a catecholate ligand. The average Os–O distance in this complex is 2.014 (3) Å, which is slightly shorter than the average Ru–O distance of 2.033 (3) Å in the corresponding Ru complex. Shorter M–O distances and longer C–O lengths in the Os complex, relative to the ruthenium analogue point to a higher oxidation state for osmium and more catechol character for the quinone ligand. The same trend has been found to be true for the tris(quinone) complexes of these metals and also for $M(bpy)_2(Q)^+$ (M = Ru, Os).[2,6,7] The green dichloromethane solution of $Os(PPh_3)_2(DBQ)Cl_2$ displays several bands in the near-IR, visible, and UV regions (Figure 3; Table V). The low intensity

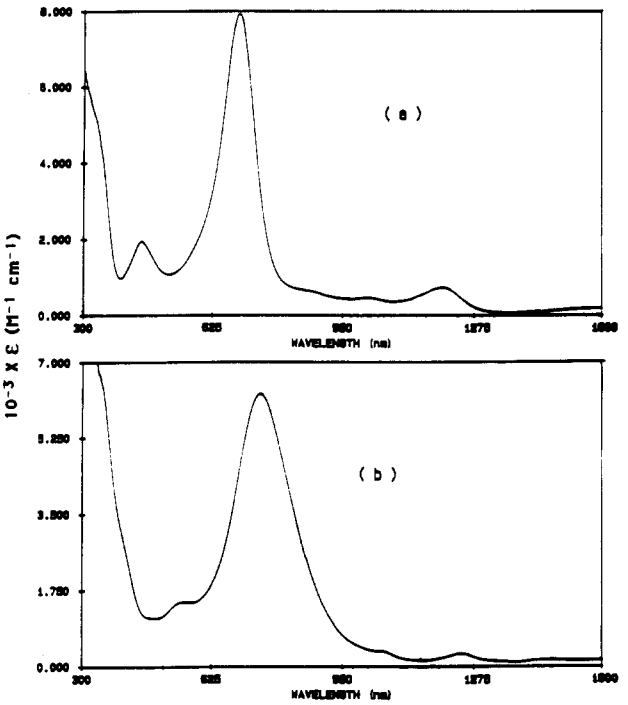

Figure 3. Visible and near-IR absorption spectra of (a) $Os(PPh_3)_2(DBQ)Cl_2$ and (b) $Os(PPh_3)_2(Cl_4Q)Cl_2$ in dichloromethane solution.

Table V. Electronic Spectral Data in Dichloromethane Solution

compd	λ, nm (ε, M^{-1}, cm^{-1})
$Os(PPh_3)_2(DBQ)Cl_2$	1195 (750), 1008 (480), 695 (7900), 448 (1900), 348[a] (5500), 262 (26 600), 238 (30 500)
$Os(PPh_3)_2(Cl_4Q)Cl_2$	1242 (310), 1048[a] (360), 748 (6300), 555[a] (1500), 356[a] (6500), 290 (15 000)
$Os(PPh_3)_2(DBQ)_2$	1050[a] (5000), 897 (7700), 550 (8600), 360[a] (3300), 293[a] (8700), 266[a] (14 000), 236 (31 300)
$Os(PPh_3)_2(DBQ)(Cl_4Q)$	1065[a] (1900), 866 (4900), 536 (4900), 270[a] (14 300), 234 (49 800)
$Os(PPh_3)_2(Cl_4Q)_2$	1242 (1100), 875[a] (4200), 751 (5700), 553 (3900), 410[a] (2300), 355[a] (4800), 263[a] (25 400), 240 (39 300)

[a] Shoulder.

Table VI. Cyclic Voltammetric Data

compd	$E_{1/2}$, V vs Fc/Fc^+ (ΔE_p, mV)[a]
$Os(PPh_3)_2(DBQ)Cl_2$	0.233 (220), −1.007 (260)
$Ru(PPh_3)_2(DBSQ)Cl_2$[b]	0.297 (90), −0.775 (138)
$Os(PPh_3)_2(Cl_4Q)Cl_2$	0.752 (122), −0.461 (96), −1.455 (E_{pc})
$Ru(PPh_3)_2(Cl_4SQ)Cl_2$[b]	0.821 (E_{pa}), −0.281 (80), −1.515 (E_{pc})
$Os(PPh_3)_2(DBQ)_2$	0.505 (112), −0.114 (98), −1.335 (120)
$Ru(PPh_3)_2(DBSQ)_2$[b]	0.438 (126), −0.220 (86), −1.330 (118)
$Os(PPh_3)_2(DBQ)(Cl_4Q)$	0.799 (103), 0.177 (87), −0.943 (92)
$Ru(PPh_3)_2(DBSQ)(Cl_4SQ)$[b]	0.739 (100), 0.155 (84), −0.876 (118)
$Os(PPh_3)_2(Cl_4Q)_2$	0.707 (103), 0.463 (90), −0.494 (116), −1.380 (144)
$Ru(PPh_3)_2(Cl_4SQ)_2$[b]	0.943 (87), 0.440 (82), −0.383 (80), −1.147 (108)

[a] In dichloromethane (0.1 M TBAP) solution at 23 °C; $E_{1/2}$ = half-wave potential; ΔE_p = peak separation between anodic and cathodic peaks of CV; scan rate = 100 mV/s. [b] Values obtained under similar experimental conditions.

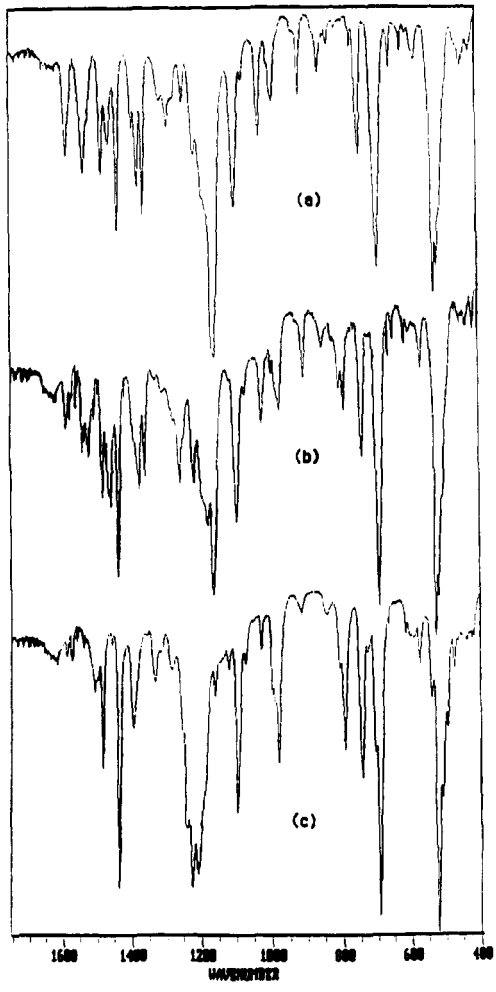

Figure 4. Infrared spectra of (a) $Os(PPh_3)_2(DBQ)_2$, (b) $Os(PPh_3)_2(DBQ)(Cl_4Q)$ and (c) $Os(PPh_3)_2(Cl_4Q)_2$.

bands at 1195 and 1008 nm may be assigned to d–d transitions.[11] Cyclic voltammograms recorded on $Os(PPh_3)_2(DBQ)Cl_2$ in dichloromethane solution show one oxidation and one reduction (Table VI). Both processes are believed to be primarily ligand-based since a positive shift of about 500 mV has been observed for both processes upon changing the quinone ligand from DBQ to Cl_4Q.[12] $Ru(PPh_3)_2(DBSQ)Cl_2$ showed similar redox properties in solution, indicating that the related complexes of both metals probably have similar charge distributions in solution.

$Os(PPh_3)_2(Cl_4Q)Cl_2$. This diamagnetic complex has been synthesized by addition of Cl_4BQ to $Os(PPh_3)_3Cl_2$ in dichloromethane with simultaneous displacement of one PPh_3 ligand. The IR-spectrum of $Os(PPh_3)_2(Cl_4Q)Cl_2$ (Figure 1) shows that the quinone ligand is bonded in reduced form. The electronic spectrum was recorded on a green dichloromethane solution of this compound. Data are given in Table V and a selected portion of the spectrum is shown in Figure 3. Two low-intensity bands were observed at 1242 and 1048 nm, similar to those observed for $Os(PPh_3)_2(DBQ)Cl_2$, which may be assigned to d–d transitions. Cyclic voltammetric studies on this complex show one oxidation and two reductions (Table VI). Values of potentials for the oxidation and first reduction are shifted positively by about 500 mV relative to those observed for $Os(PPh_3)_2(DBQ)Cl_2$. This indicates that these two electrochemical processes are ligand-centered. The second reduction is probably metal-centered and was not observed for $Os(PPh_3)_2(DBQ)Cl_2$ within the voltage window offered by dichloromethane. Potentials for all three couples for $Os(PPh_3)_2(Cl_4Q)Cl_2$ compare well with those observed for $Ru(PPh_3)_2(Cl_4SQ)Cl_2$ (Table VI), indicating a similar charge distribution in solution. Similarities in the spectroscopic and electron-transfer properties within the $M(PPh_3)_2(Q)Cl_2$ (M = Ru, Os; Q = DBQ, Cl_4Q) series suggest that the charge distribution in solution is the same for the four complexes.

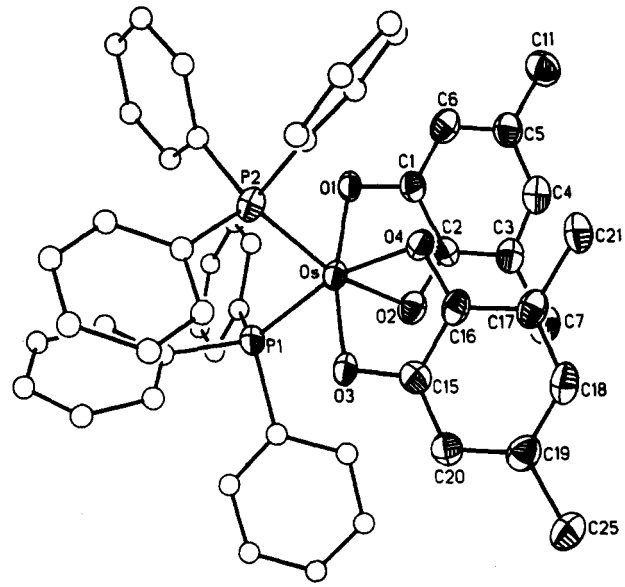

Figure 5. View of the $Os(PPh_3)_2(DBQ)_2$ complex molecule.

Table VII. Selected Bond Distances and Angles for $Os(PPh_3)_2(DBQ)_2$

	Distances (Å)		
Os–P1	2.357 (2)	Os–P2	2.350 (2)
Os–O1	2.001 (4)	Os–O3	1.982 (4)
Os–O2	2.048 (5)	Os–O4	2.042 (4)
C1–O1	1.326 (8)	C15–O3	1.341 (8)
C2–O2	1.321 (7)	C16–O4	1.333 (7)
C1–C2	1.407 (8)	C15–C16	1.422 (9)
C2–C3	1.423 (10)	C16–C17	1.414 (9)
C3–C4	1.365 (9)	C17–C18	1.394 (9)
C4–C5	1.409 (10)	C18–C19	1.390 (9)
C5–C6	1.378 (11)	C19–C20	1.380 (10)
C6–C1	1.402 (9)	C20–C15	1.396 (9)
	Angles (deg)		
P1–Os–P2	98.8 (1)	P1–Os–O1	104.3 (1)
P2–Os–O1	86.6 (1)	P1–Os–O2	90.8 (1)
P2–Os–O2	164.6 (1)	O1–Os–O2	79.4 (2)
P1–Os–O3	85.7 (1)	P2–Os–O3	101.0 (1)
O1–Os–O3	166.5 (2)	O2–Os–O3	91.6 (2)
P1–Os–O4	164.7 (1)	P2–Os–O4	90.1 (1)
O1–Os–O4	88.6 (2)	O2–Os–O4	83.5 (2)
O3–Os–O4	80.3 (2)		

$Os(PPh_3)_2(DBQ)_2$. This bis(quinone) compound can be synthesized either by direct reaction of H_2DBCat with $Os(PPh_3)_3Cl_2$ in refluxing ethanol or by displacement of two chloride ligands from $Os(PPh_3)_2(DBQ)Cl_2$ with $DBCat^{2-}$ in a refluxing dichloromethane/ethanol solution. This compound is diamagnetic and displays sharp ^1H NMR signals for the *tert*-butyl protons at 0.672 and 1.282 ppm, indicating the presence of one isomer in solution. Three different localized charge distributions, $Os^{II}(SQ)_2$, $Os^{III}(SQ)(Cat)$ and $Os^{IV}(Cat)_2$ are possible for this complex. The IR spectrum of $Os(PPh_3)_2(DBQ)_2$ (Figure 4) shows features observed in the spectrum of $Os(PPh_3)_2(DBQ)Cl_2$, the major difference being appearance of an additional intense band at 1159 cm^{-1} in the former complex. This complex has been characterized X-ray crystallographically. A view of the $Os(PPh_3)_2(DBQ)_2$ molecule is shown in Figure 5 and selected bond distances and angles are given in Table VII. PPh_3 ligands are cis to one another in the complex molecule, C–O lengths for one ligand are 1.326 (8) and 1.321 (7) Å, values which lie in between catecholate and semiquinonate C–O lengths. For the second ligand the two C–O lengths are 1.341 (8) and 1.333 (7) Å, values typically found for

(11) Lahiri, G. K.; Bhattacharya, S.; Ghosh, B. K.; Chakravorty, A. *Inorg. Chem.* **1987**, *26*, 4324.
(12) Bradbury, J. R.; Schultz, F. A. *Inorg. Chem.* **1986**, *25*, 4416.

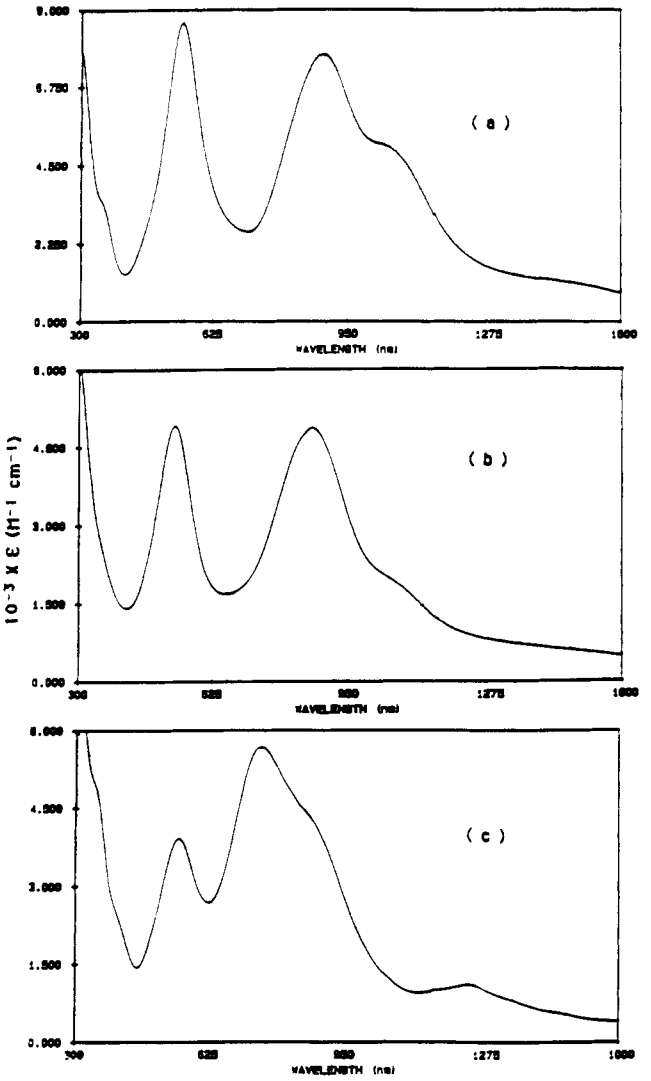

Figure 6. Visible and near-IR absorption spectra of (a) $Os(PPh_3)_2(DBQ)_2$, (b) $Os(PPh_3)_2(DBQ)(Cl_4Q)$, and (c) $Os(PPh_3)_2(Cl_4Q)_2$ in dichloromethane solution.

catecholate ligands. The Os–O distances show a regular pattern. The shortest Os–O distance is to the quinone oxygen with the longest C–O bond length (Table VII). The charge distribution for $Os(PPh_3)_2(DBQ)_2$ in solid appears typical of a $Os^{IV}(Cat)_2$ species. The dichloromethane solution of this compound is purple and displays several intense bands in the near-IR, visible, and UV regions (Figure 6; Table V). Cyclic voltammograms recorded in dichloromethane solution show three reversible redox processes, two oxidations and one reduction (Figure 7; Table VI). The values of potentials for the redox couples compare well with those observed for $Ru(PPh_3)_2(DBSQ)_2$, which indicates that in solution a correspondence exists between electronic energy levels of the osmium and ruthenium complexes.

$Os(PPh_3)_2(DBQ)(Cl_4Q)$. The reaction of $Os(PPh_3)_2(DBQ)Cl_2$ with H_2Cl_4Cat in the presence of NEt_3 in refluxing dichloromethane ethanol afforded $Os(PPh_3)_2(DBQ)(Cl_4Q)$ as a purple solid. $Os(PPh_3)_2(DBQ)(Cl_4Q)$ is diamagnetic and displays two sets of sharp ^1H NMR signals for the *tert*-butyl protons at 0.672 and 1.302 ppm and at 0.755 and 1.324 ppm of approximate intensity ratio 3:1, indicating existence of two isomers in solution. The IR spectrum contains features of both DBQ and Cl_4Q ligands (Figure 4). Electronic spectra recorded in dichloromethane solution show intense bands in the near-IR, visible, and UV regions (Table V; Figure 6). Electron-transfer properties were studied by cyclic voltammetry in dichloromethane solution. Two oxidations and one reduction are observed (Table VI) at potentials comparable to those of corresponding redox processes of the analogous ruthenium complex, which may indicate that the two

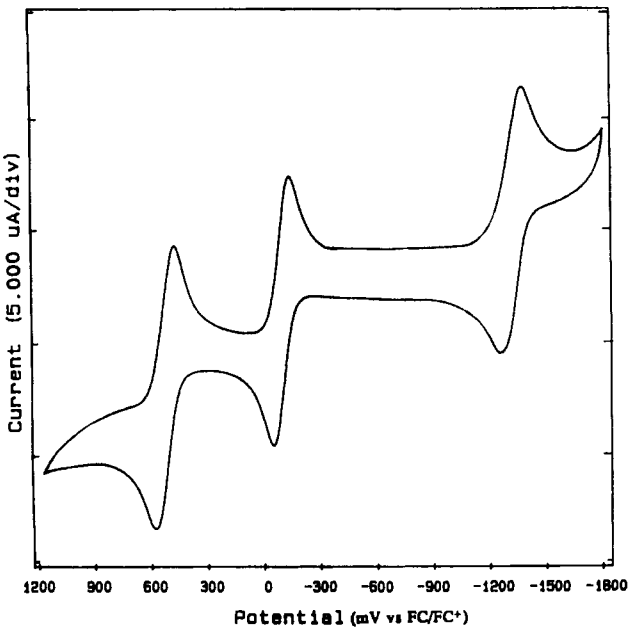

Figure 7. Cyclic voltammogram of $Os(PPh_3)_2(DBQ)_2$ recorded in dichloromethane (0.1 M TBAP) solution at a scan rate of 100 mV/s.

complexes have a similar charge distribution in solution.

$Os(PPh_3)_2(Cl_4Q)_2$. This compound is obtained in good yield as a purple diamagnetic solid from the reaction of H_2Cl_4Cat with $Os(PPh_3)_3Cl_2$ in refluxing ethanol. The IR-spectrum of $Os(PPh_3)_2(Cl_4Q)_2$ (Figure 4) shows features that are similar to those observed in the spectrum of $Os(PPh_3)_2(Cl_4Q)Cl_2$. In dichloromethane solution the complex shows a number of intense bands in the near-IR, visible, and UV regions. Electronic spectral data are given in Table V and a selected region of the spectrum is shown in Figure 6. Cyclic voltammetry in dichloromethane solution shows four redox couples (Table VI): two oxidations and two reductions. Values of potentials for all the four couples are similar to those observed for $Ru(PPh_3)_2(Cl_4SQ)_2$. This indicates that the same correspondence exists in solution for the bis(tetrachloroquinone) complexes of osmium and ruthenium as was noted for the bis(di-*tert*-butylquinone) complexes and the mixed-quinone-ligand complexes.

Discussion

The $Os(PPh_3)_2(Q)Cl_2$ and $Os(PPh_3)_2(Q)_2$ (Q = DBQ, Cl_4Q) series have been studied in the solid state and in solution. It is of interest to compare these results with the properties of their ruthenium analogues. Structural characterization on both $Ru(PPh_3)_2(DBSQ)Cl_2$[8] and $Os(PPh_3)_2(DBSQ)Cl_2$ has shown that the ruthenium complex appears more like a Ru(III)–semiquinone species while the quinone ligand of the osmium analogue appears more catechol-like. Shorter Os–O lengths also point to a higher oxidation state for the metal; however, the structural features of the quinone are not strictly typical of a catecholate ligand. A similar result was found for the $[M(bpy)(Q)]^+$ (M = Ru, Os) series where it appeared to reflect differences in metal–quinone charge delocalization.[7] The properties of $Os(PPh_3)_2(Q)Cl_2$ (Q = DBQ, Cl_4Q) in dichloromethane solution show features that are more in agreement with the M(III)–SQ charge distribution assigned to $Ru(PPh_3)_2(DBSQ)Cl_2$ on the basis of its crystal structure. Two low-energy transitions are observed in the near-infrared spectra of both complexes that are typical in energy and intensity of d–d transitions between the states that arise from the spin–orbit coupling effects of Os(III).[11] The electrochemistry on $Ru(PPh_3)_2(DBSQ)Cl_2$ and $Os(PPh_3)_2(DBSQ)Cl_2$ can be assigned by recognizing that metal-based redox processes of third-row metals occur at more negative potentials than corresponding couples of second-row metals. The reduction for the complexes listed in Table VI may be associated with a M(III)/M(II) process and the oxidation would therefore correspond to a BQ/SQ couple for the quinone ligand. The electrochemical properties of the

$M(PPh_3)_2(Cl_4Q)Cl_2$ (M = Ru, Os) complexes are more difficult to assign. Redox processes of the tetrachloroquinone ligand occur at potentials that are approximately 0.5 V more positive than the corresponding potentials of the DBQ ligand.[12] The first reduction of $Os(PPh_3)_2(Cl_4Q)Cl_2$ shows the shift relative to its Ru analogue, which may be characteristic of a M(III)/M(II) couple. Yet the reductions of both the Ru and Os complexes are shifted positively relative to those of their DBQ analogues in a way that would suggest that they are quinone ligand-based. Similar ambiguities existed in the assignment of couples of the $[M(bpy)_2(Q)]^+$ (M = Ru, Os; Q = DBCat, Cat, Cl_4Cat) series.[7] The problem may be understood by recognizing that the electronic levels responsible for electrochemical activity represent combinations of metal and quinone ligand orbital contributions. The shift from Ru to Os or from DBQ to ClQ may result in changes in orbital composition that give rise to apparently irrational shifts in electrochemical potentials. The conclusion from this characterization is that metal–quinone delocalization contributes to the electronic structure of the $M(PPh_3)_2(Q)Cl_2$ redox series in much the same way that it appeared for the $M(bpy)_2(Q)$ series.

Structural characterization on $Os(PPh_3)_2(DBQ)_2$ shows that the trend toward shorter M–O bond lengths and longer ligand C–O lengths found for the $ML_4(Q)$ and $M(Q)_3$ series of Ru and Os complexes is carried over to the $M(PPh_3)_2(Q)_2$ series. The complex in the solid state appears to be a bis(catecholate) complex of Os(IV) while structural characterization of $Ru(PPh_3)_2(Cl_4SQ)_2$ showed ligand structural features that were typically semiquinone.[8] Spectral and electrochemical similarities between corresponding members of the series $Ru(bpy)(Q)_2$ and $Ru(PPh_3)_2(Q)_2$ series led to the conclusion that the electronic levels associated with these properties were insensitive to metal orbital energy and that, in solution, the electronic structure of these complexes was the result of interligand delocalization.[8] Comparison of the corresponding members of M $Os(PPh_3)_2(Q)_2$ series with M = Ru and Os offers the opportunity to extend this investigation. Spectra listed in Table V and shown in Figure 6 bear close resemblance, particularly in the visible and near-infrared regions, to spectra of corresponding Ru complexes. Electrochemical potentials listed in Table VI show the same progressive shift in the positive direction from $Os(PPh_3)_2(DBQ)_2$ to the mixed-ligand complex, $Os(PPh_3)_2(DBQ)(Cl_4Q)$, and to $Os(PPh_3)_2(Cl_4Q)_2$. Further, the information in Table VI shows the close correspondence between related couples for the Ru and Os complexes. This observation serves to reinforce the view that metal orbital contributions to the frontier orbital structure of the $M(PPh_3)_2(Q)_2$ (M = Ru, Os) and $Ru(bpy)(Q)_2$ series are quite small. A more detailed comparison of these effects will be presented once studies on the $Os(bpy)(Q)_2$ series are complete.

Acknowledgment. This research was supported by the National Science Foundation under Grant CHE 88-09923. Ruthenium trichloride was provided by Johnson Matthey, Inc. through their Metal Loan Program.

Supplementary Material Available: For $Os(PPh_3)_2(DBQ)Cl_2$ and $Os(PPh_3)_2(DBQ)_2$, tables giving crystal data and details of the structure determination, atom coordinates, bond distances and angles, anisotropic thermal parameters, and hydrogen atom locations (26 pages); listings of observed and calculated structure factors for both compounds (33 pages). Ordering information is given on any current masthead page.

Contribution from the Departments of Chemistry, Montana State University, Bozeman, Montana 59717, and Western New Mexico University, Silver City, New Mexico 88061

Vitamin B_6 Model Reactions. 4. Stereoelectronic Catalysis of Carbon–Hydrogen Bond-Breaking Reactions and Crystal and Molecular Structure of Tetramethylammonium Bis(pyridoxylideneglycinato)cobaltate(III)–4.5-Water

Andrew G. Sykes,† Raymond D. Larsen,† James R. Fischer,‡ and Edwin H. Abbott*,†

Received July 18, 1990

The anionic complex bis(pyridoxylideneglycinato)cobaltate(III) holds the pyridoxal (vitamin B_6) Schiff base of glycine in a fixed conformation. Rates of carbon–hydrogen bond breaking have been measured for the diastereotopic protons of the glycine moiety's methylene group. Nuclear magnetic resonance measurements show that the fastest exchange occurs for the proton whose C–H bond is more nearly dihedrally perpendicular to the plane of the π system in the aromatic ring. Activation parameters are reported, and $\Delta H^{\ddagger}$ is found to be reduced for the more rapidly exchanging proton. The structure of the anion was determined by the X-ray crystallography of its tetramethylammonium salt, providing further insight into the factors responsible for the differential reactivity of the methylene protons. Crystallographic data are as follows: $P\bar{1}$, a = 8.545 (5) Å, b = 12.761 (6) Å, c = 14.158 (8) Å, α = 98.85 (4)°, β = 94.95 (5)°, γ = 91.08 (4) Å, V = 1519 (1) Å^3, Z = 2 (R = 0.090, R_w = 0.088).

Introduction

Vitamin B_6, in one of its forms, is the heterocyclic aldehyde pyridoxal (I). It is an essential cofactor to a large number of enzymes that catalyze many diverse reactions of amino acids.[1]

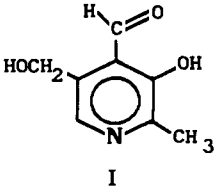

I

These reactions are known to proceed through Schiff base formation at the enzyme active site and are simply formulated as proceeding through Snell–Braunstein electron shifts into the pyridine ring as indicated in II. Accordingly, reactions are

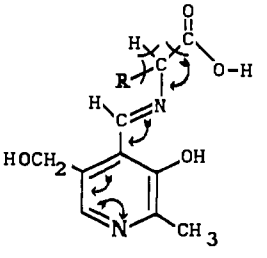

II

formulated as beginning by breaking one of the three bonds to the amino acid α-carbon atom. Some years ago, Dunathan hypothesized that the enzyme could select the bond to be broken

† Montana State University.
‡ Western New Mexico University.

(1) (a) Metzler, D. E.; Ikawa, M.; Snell, E. E. *J. Am. Chem. Soc.* **1954**, *76*, 648. (b) Martell, A. E. *Adv. Enzymol. Relat. Areas Mol. Biol.* **1982**, *53*, 163.

0020-1669/91/1330-2911$02.50/0